Remote Sensing of Environment 287 (2023) 113479

Contents lists available at ScienceDirect

Remote Sensing of Environment

journal homepage: www.elsevier.com/locate/rse

Atmospheric humidity and temperature sounding from the CubeSat TROPICS mission: Early performance evaluation with MiRS

John Xun Yang [a,b,*], Yong-Keun Lee [a,b], Christopher Grassotti [a,b], Kevin Garrett [b], Quanhua Liu (Mark)[b], William Blackwell [c], R. Vincent Leslie [c], Tom Greenwald [d], Ralf Bennartz [e], Scott Braun [f]

[a] Cooperative Institute for Satellite Earth System Studies, Earth System Science Interdisciplinary Center, University of Maryland, College Park, MD, USA
[b] NOAA Center for Satellite Applications and Research, National Environmental Satellite, Data, and Information Service, College Park, MD, USA
[c] MIT Lincoln Laboratory, Lexington, MA, USA
[d] Cooperative Institute for Meteorological Satellite Studies, University of Wisconsin—Madison, Madison, WI, USA
[e] Earth and Environmental Sciences Department, Vanderbilt University, Nashville, TN, USA
[f] NASA Goddard Space Flight Center, Greenbelt, MD, USA

ARTICLE INFO

Edited by Dr. Menghua Wang

Keywords:
Atmospheric sounding
Microwave radiometry
Moisture and temperature
CubeSat
TROPICS
MiRS

ABSTRACT

Atmospheric humidity and temperature are the two most important geophysical variables for numerical weather forecasting and relevant Earth studies, contributing to the reduction of over 60% forecast errors. Conventional large satellite microwave radiometers provide the primary sounding data of moisture and temperature, with the V-band (near 50 GHz) and G-band (near 183 GHz) as the main spectra. In recent years, CubeSats are rapidly developing with compact sizes, novel designs, and low cost. The NASA TROPICS is an ongoing CubeSat constellation mission for studying tropical meteorology and storm systems, with the first Pathfinder satellite launched on 30 June 2021, which will provide a median revisit rate better than 60 min. TROPICS has innovative channels at F-band (near 118 GHz) and 205 GHz, providing a new perspective for atmospheric sounding. In this study, we have extended the NOAA MiRS system and applied it to TROPICS Pathfinder early-phase, provisionally calibrated data, focusing on moisture and temperature. We have examined the retrieval quality and compared with the ECMWF analysis and MiRS retrievals from NOAA-20 ATMS. An experiment of subsetting ATMS to match up with TROPICS channels is also conducted. Here we focus on atmospheric humidity and temperature retrievals, since they are of primary importance for microwave sounders and is tied to the core of the TROPICS mission along with precipitation retrieval. Compared to traditional channels, TROPICS F-band and 205 GHz provide new information content with distinct sensitivity to moisture and hydrometeors, showing for example over 20 K larger dynamic range of brightness temperature at 205 GHz compared to 190 GHz. The retrieved total precipitable water compared to ECMWF has a correlation coefficient of 0.955, 0.985, and 0.977 for TROPICS, ATMS, and ATMS subset, respectively. For water vapor profile, the standard deviation of retrieval to ECMWF is 0.93, 0.76, and 0.80 g/kg for the three experiments, respectively, and regarding temperature, it is 2.5, 1.5, and 1.6 K, respectively. The retrieval shows dependence on surface type and clouds, where land and cloudy conditions degrade retrieval compared to ocean and clear condition. The early performance is promising, and the successful MiRS extension paves the way to explore improved data when the calibration validation is complete and from the forthcoming constellation.

1. Introduction

Atmospheric humidity and temperature sounding are indispensable in weather, climate and environmental science, contributing to over 60% in reducing weather forecast errors in terms of forecast sensitivity to observation impact (Joo et al., 2013; Geer et al., 2017). The humidity and temperature are associated with and affect a range of geophysical variables and processes such as precipitation, clouds and radiation. The monitoring and forecasting for natural disasters such as hurricanes (Kidder et al., 2000), heat waves (Kunkel et al., 1996), and wildfires

* Corresponding author at: Cooperative Institute for Satellite Earth System Studies, Earth System Science Interdisciplinary Center, University of Maryland, College Park, MD, USA.
E-mail address: jxyang@umd.edu (J.X. Yang).

https://doi.org/10.1016/j.rse.2023.113479
Received 21 September 2022; Received in revised form 19 December 2022; Accepted 19 January 2023

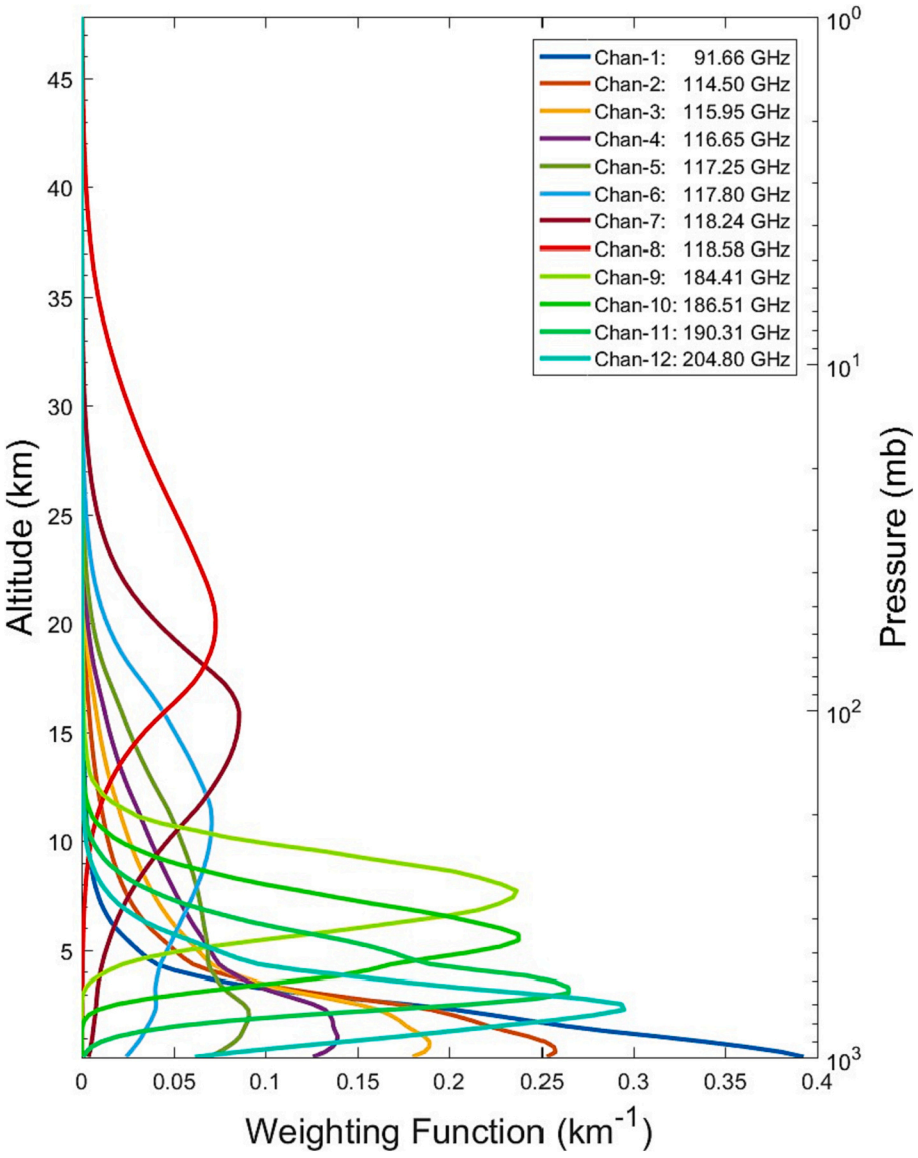

Fig. 1. Weighting function of TROPICS channels in tropical regions.

(Levin and Heimowitz, 2012) also need moisture and temperature as critical state variables. Among all conventional and remote sensing instruments, satellite microwave radiometry dominates in reducing forecast error of ~40% with essential moisture and temperature information, taking advantage of dense global coverage under all-weather conditions (Joo et al., 2013; Geer et al., 2017). There are currently a series of in-orbit microwave sounders in support of weather and environmental services at the National Oceanic and Atmospheric Administration (NOAA) and the European Organization for the Exploitation of Meteorological Satellites (EUMETSAT).

While microwave sounders onboard large satellites have been the backbone in sounding and continue to backup weather and environmental studies, small satellites (SmallSats) are rapidly emerging (Blackwell, 2015; Marinan et al., 2016; Blackwell et al., 2018; Camps et al., 2018; Padmanabhan et al., 2020). An obvious advantage of SmallSats is improving the revisit time with constellations at a low cost. In addition, a SmallSat can take advantage of technology advancement and develop high-performance sensors with innovative design and advanced electronics. The National Aeronautics and Space Administration (NASA) has funded a number of SmallSat missions through the Earth Venture Program. The NASA **T**ime-**R**esolved **O**bservations of **P**recipitation structure and storm **I**ntensity with a **C**onstellation of **S**mallsats (TROPICS) mission aims to measure tropical meteorology, storm structure, and precipitation with a CubeSat constellation (Blackwell et al., 2018). CubeSat is a category of SmallSats and has a standard size and form factor, with one unit (1U) of 10 × 10 × 10 cm. TROPICS comprises 3U CubeSats (10 × 10 × 36 cm), each weighing only 6 kg. The payload is the TROPICS Microwave Sounder (TMS), a 12-channel total power radiometer. TROPICS is the successor of the Microsized Microwave Atmospheric Satellite (MicroMAS-2A), which is a technology demonstration CubeSat launched in 2018 (Crews et al., 2020). The median revisit rate of TROPICS is designed to be less than 60 min with four 3U CubeSats of an orbit inclination of 30 degrees and 530 km altitude. To reduce risk of the TROPICS constellation mission, an additional CubeSat, the TROPICS engineering qualification model, also called the TROPICS Pathfinder, was refurbished for flight and successfully launched into a sun-synchronous orbit on 30 June 2021. The early-phase data have been provisionally calibrated and made available for a first-cut evaluation of the instrument, laying a milestone toward the forthcoming launch of the constellation mission. Efforts are now underway to finalize and validate the calibration of TROPICS Pathfinder brightness temperature data, which should further improve upon the

Table 1
TROPICS channel specification and measured in-orbit NEDT for the TROPICS Pathfinder satellite. Matchup ATMS channels with similar weighting functions are presented.

Channel	Center Freq. (GHz)	Pol.	Bandwidth (GHz)	Footprint Nadir (km)	NEDT spec. (K)	NEDT in-orbit (K)	ATMS Channel (GHz)	ATMS NEDT (K)
1	91.655 ± 1.4	H	1	29.6	0.7	0.94	88	0.21
2	114.5	H	1	24.1	1.0	0.64	50.3	0.32
3	115.95	H	0.8	24.1	0.9	0.60	51.76	0.22
4	116.65	H	0.6	24.1	0.9	0.68	52.8	0.22
5	117.25	H	0.6	24.1	0.9	0.61	53.596 ± 0.115	0.24
6	117.8	H	0.5	24.1	0.9	0.64	54.4	0.22
7	118.24	H	0.38	24.1	0.9	0.70	55.5	0.24
8	118.58	H	0.3	24.1	1.0	0.83	57.2903 ± 0.217	0.46
9	184.41	V	2	16.1	1.0	0.55	183 ± 1	0.58
10	186.51	V	2	16.1	0.6	0.57	183 ± 3	0.40
11	190.31	V	2	16.1	0.6	0.51	183 ± 7	0.35
12	204.8	V	2	15.6	0.6	0.59	165.5	0.32

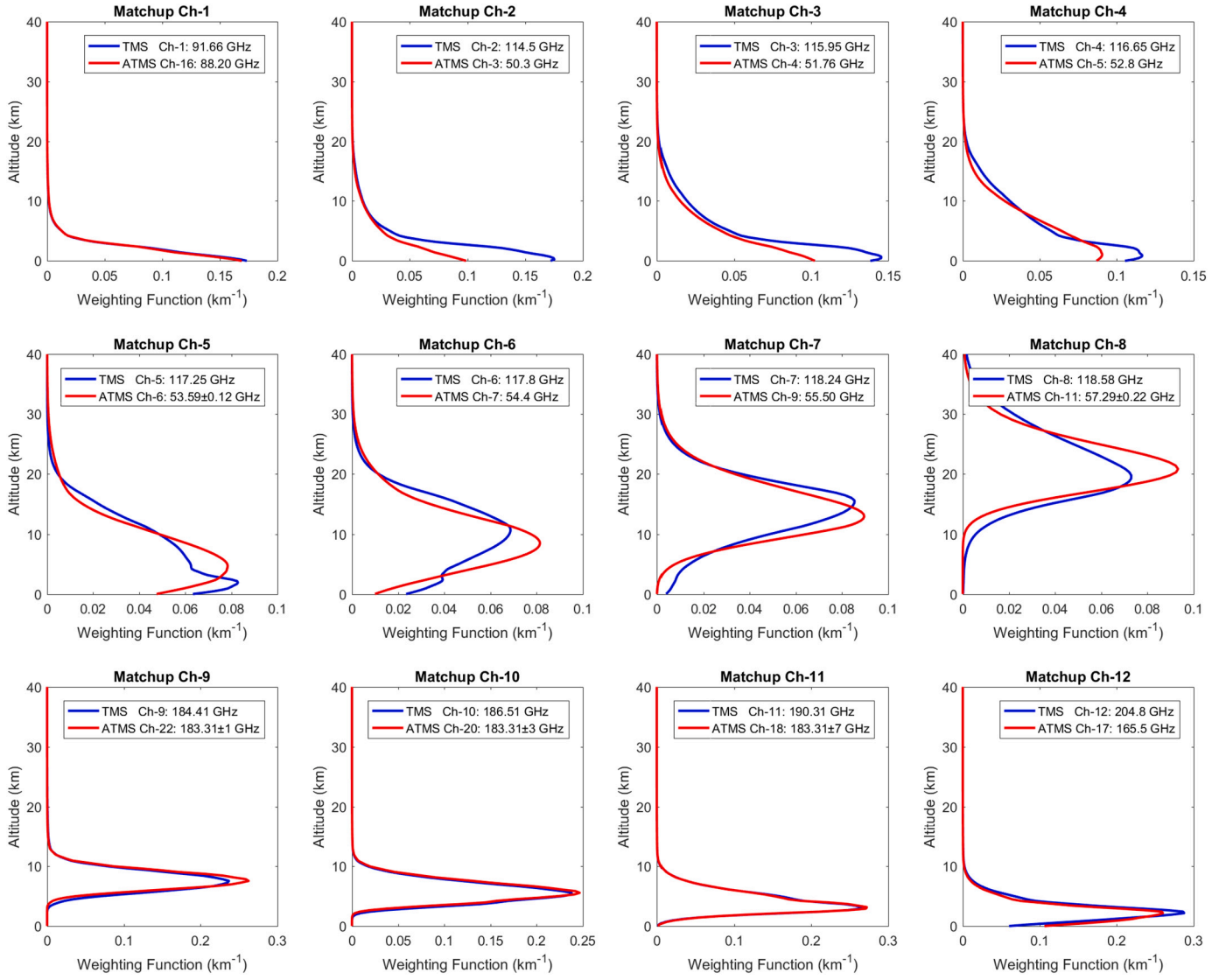

Fig. 2. Weighting function of matchup channels between TROPICS TMS and N20 ATMS. Apart from using all ATMS channels, the ATMS subset channels will also be used in retrieval for comparison.

results presented in this paper.

As opposed to conventional satellite microwave sounders relying on G-band (near 183 GHz) and V-band (near 50 GHz) for humidity and temperature sounding, TROPICS utilizes new frequencies. Conventional G-band channels have an upper bound at 190 GHz (183 ± 7 GHz) (Saunders et al., 1995; Kim et al., 2022; Yang et al., 2022), whereas

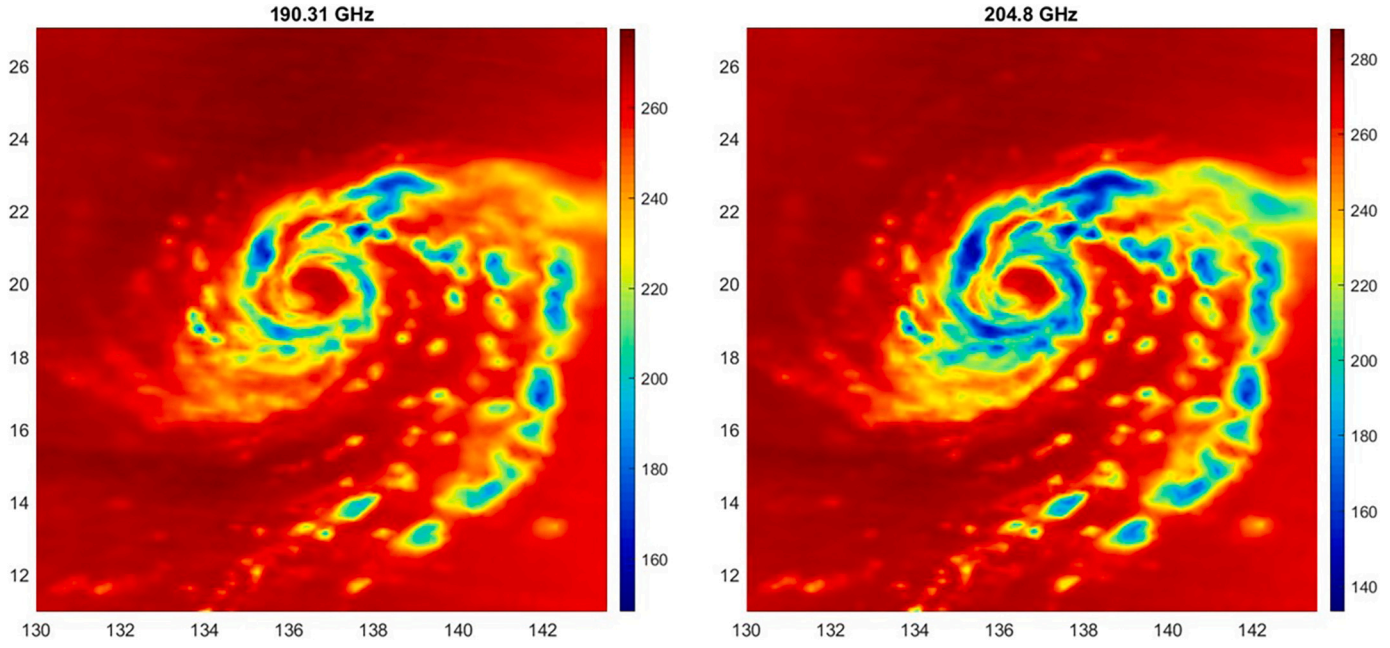

Fig. 3. Typhoon Mindulle at 5:10 UTC on 27 September 2021 captured at channel 11 (190.31 GHz) and 12 (204.8 GHz) of TROPICS. The brand new 204.8 GHz provides an unprecedented view of Mindulle with a large brightness temperature range of 155 K. In comparison, the brightness temperature range is 129 K at 190 GHz. The eye and rainbands of Mindulle show finer structures at 204.8 GHz.

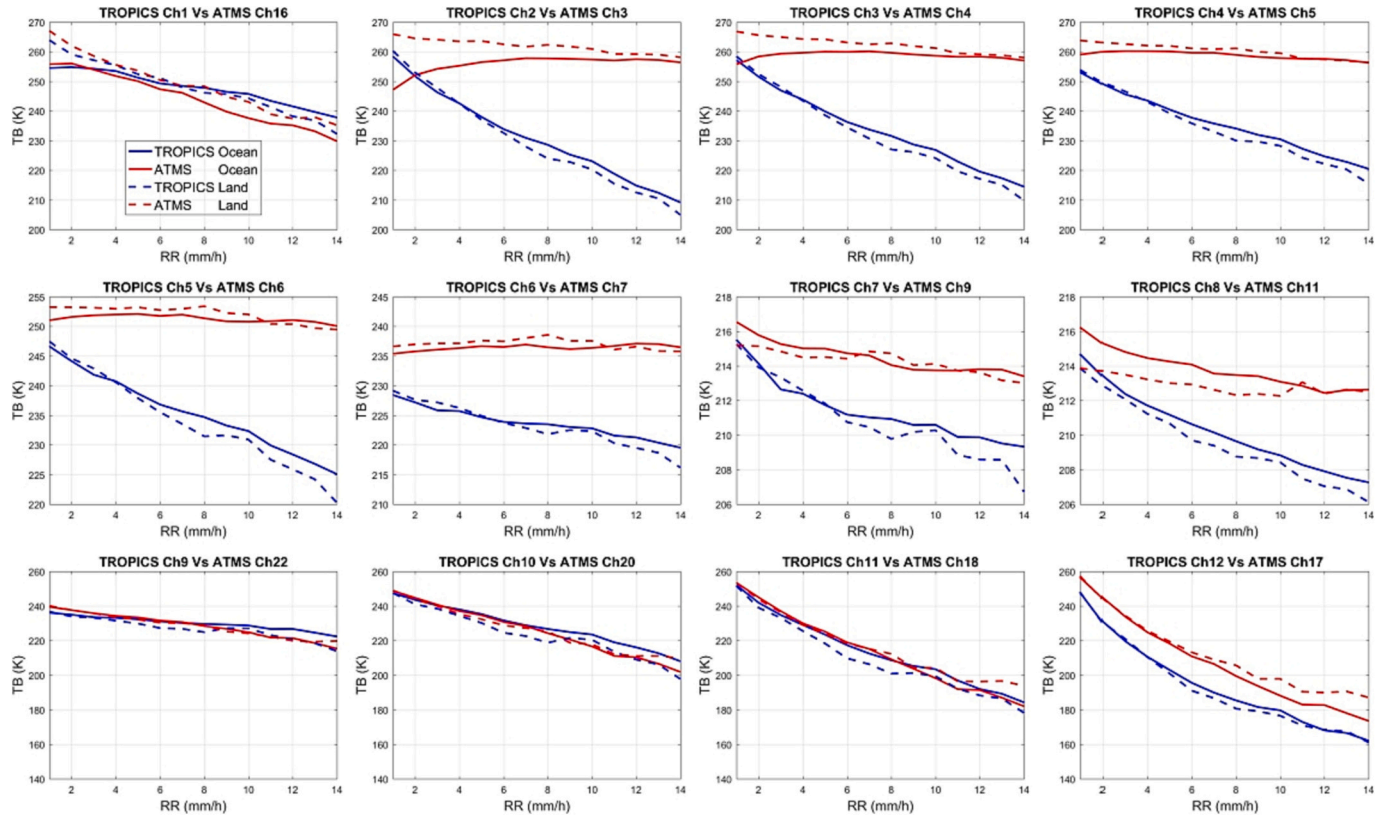

Fig. 4. TROPICS TB sensitivity to rain rate. Coincident channels of NOAA-20 ATMS with similar weighting functions are compared. TROPICS channels show higher sensitivity at F-band and 205 GHz, compared to corresponding V-band and G-band channels of ATMS.

TROPICS and its predecessor MicroMAS-2A have a new 205 GHz channel plus three other G-band channels (Blackwell et al., 2018; Crews et al., 2020). The 205 GHz channel is the first to be deployed in space and is expected to be more sensitive to hydrometeors due to its short wavelength. Also, TROPICS has seven channels at F-band (near 118 GHz). TROPICS and MicroMAS-2A are the first CubeSat using F-band for sounding, which is second only to the Micro-Wave Humidity Sounder-2 (MWHS-2) onboard the large satellite Feng-Yun (FY) 3C&D&E (Yang

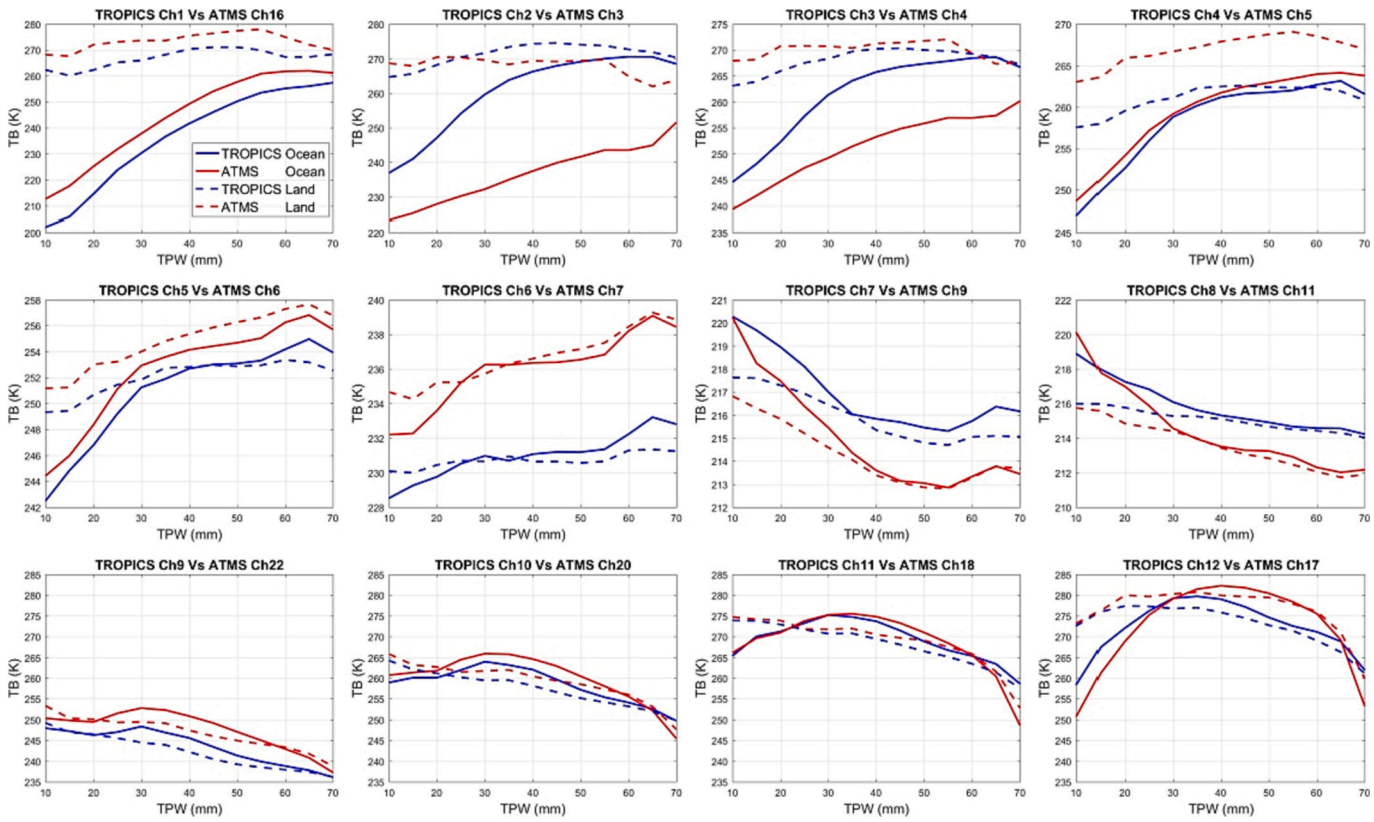

Fig. 5. TROPICS TB sensitivity to TPW. The sensitivity is especially distinct at TROPICS F-band and 205 GHz, compared to counterpart frequencies of NOAA-20 ATMS.

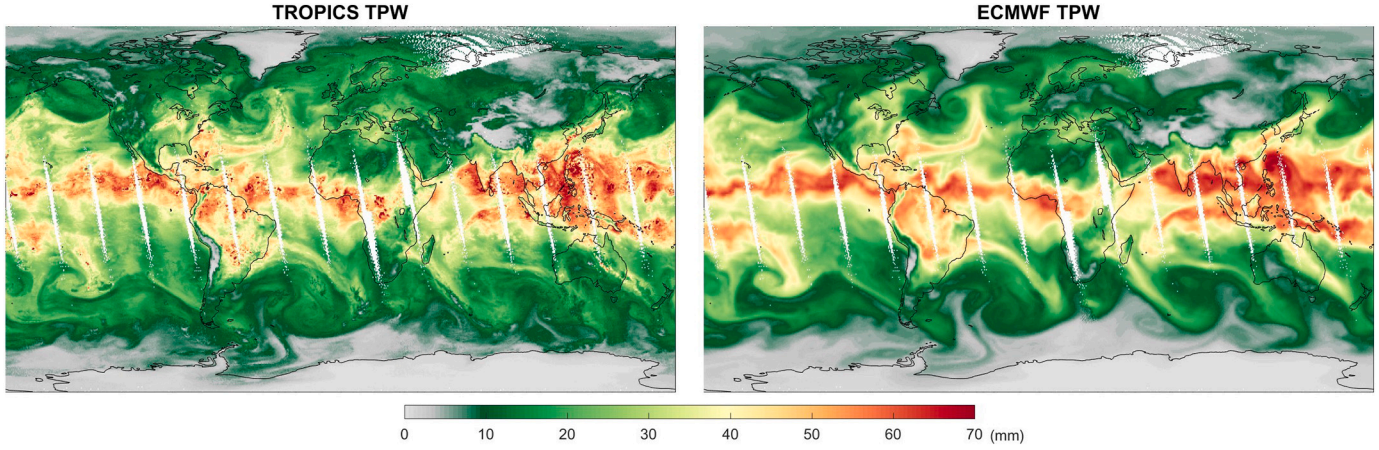

Fig. 6. Retrieved TPW (left) compared with the ECMWF analysis (right) on 10 October 2021, showing satisfactory consistency.

et al., 2012; Kan et al., 2020; Mao et al., 2022). The 205 GHz of TROPICS is among the fast development of spaceborne millimeter and sub-millimeter microwave radiometers, which have advantages in studying cloud ice, snow, and arctic weather and climate, including the Ice Cloud Imager (183–664 GHz), Microwave Sounder (with a 229 GHz channel) in the MetOp Second-Generation (Metop-SG) mission, and the Arctic Weather Satellite mission (50–325 GHz) (D'Addio et al., 2014; Lagaune et al., 2021). F-band frequencies have also gained interest, given the shorter wavelength that appears more hydrometeor-sensitive than V-band. This is why future missions such as the MetOp-SG have planned on adding F-band channels into its Microwave Imager (MWI) as well (D'Addio et al., 2014). Furthermore, TROPICS has other innovative designs: its polarization is purely V or H due to the cross-track scanning of the whole receiver, different from the mixed V and H polarization of conventional sounders that rotate a reflector instead. The use of noise diodes as warmload and single-side-band without a local oscillator is also an interesting innovation when compared with most traditional sounders (Blackwell et al., 2018).

Here we present the early performance evaluation of TROPICS Pathfinder data for atmospheric humidity and temperature sounding. The Microwave Integrated Retrieval System (MiRS) developed at NOAA is used for TROPICS retrieval (Boukabara et al., 2011). MiRS is a state-of-the-art 1D variational (1DVAR) algorithm to retrieve atmospheric and surface information from satellite passive microwave measurements. It has been supporting NOAA's operational tasks and scientific research, covering heritage and in-orbit microwave sensors of NOAA

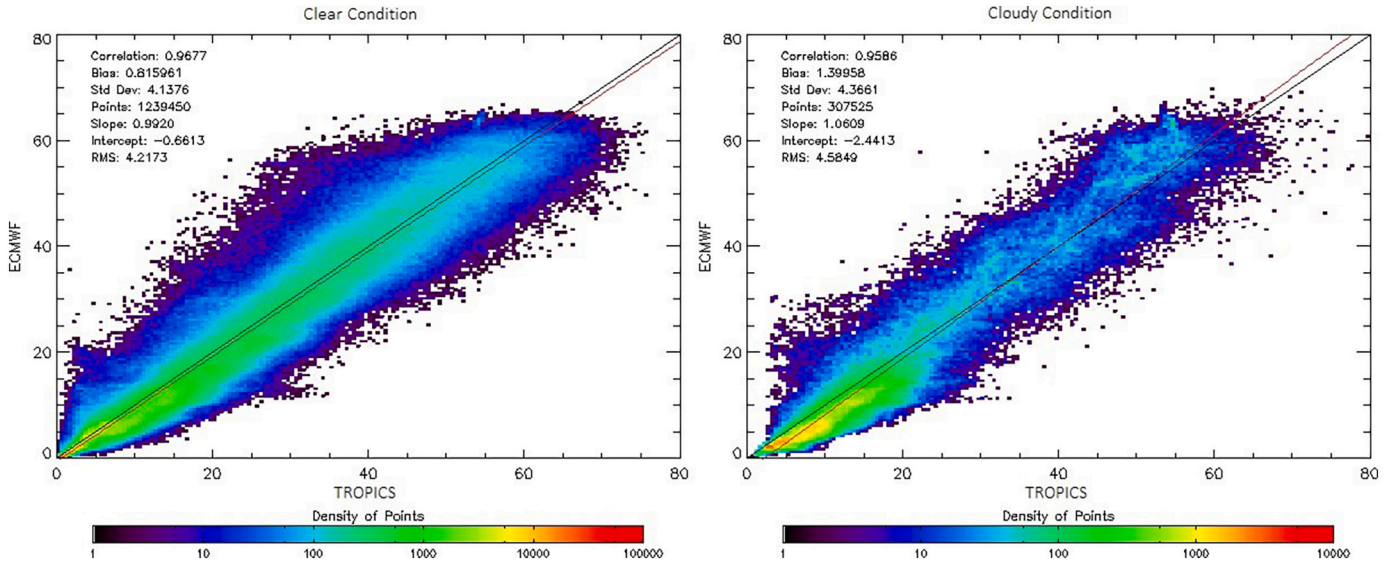

Fig. 7. Comparison of retrieved TROPICS TPW against ECMWF under (left) clear and (right) cloudy conditions. TPW performance has a correlation over 0.95 under both conditions.

Table 2
TROPICS and NOAA-20 TPW statistics against ECMWF.

Condition	Clear				Cloudy			
	Corr.	STD	Bias	No.	Corr.	STD	Bias	No.
TROPICS TMS	0.968	4.138	0.816	1239450	0.959	4.366	1.399	307525
NOAA-20 ATMS	0.989	2.527	1.256	1156236	0.979	3.115	0.757	323303
NOAA-20 ATMS subset	0.983	3.097	1.416	1266007	0.971	3.808	1.723	210270

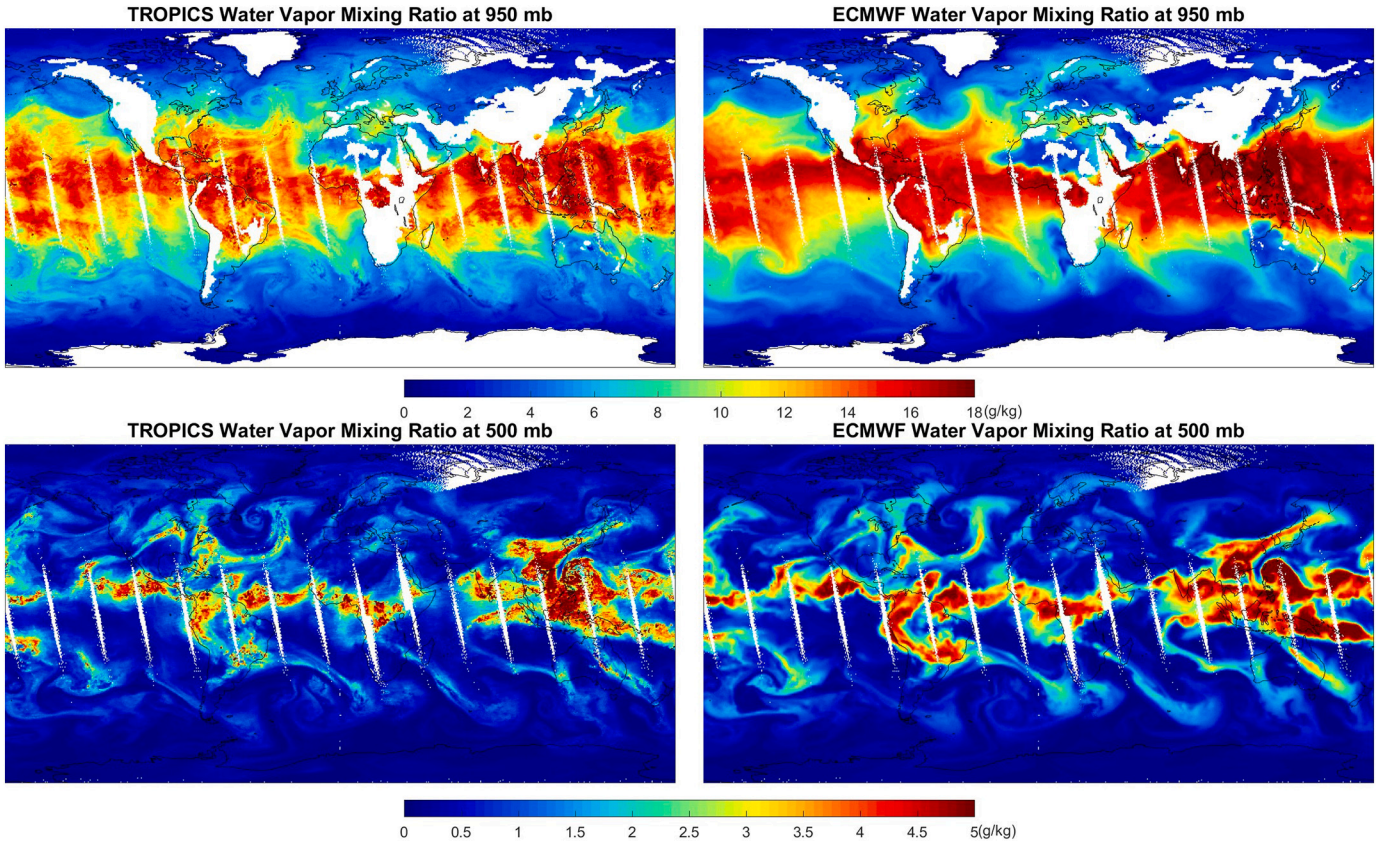

Fig. 8. Retrieved TROPICS water vapor mixing ratio at 950 and 500 hPa compared with the ECMWF analysis on 10 October 2021.

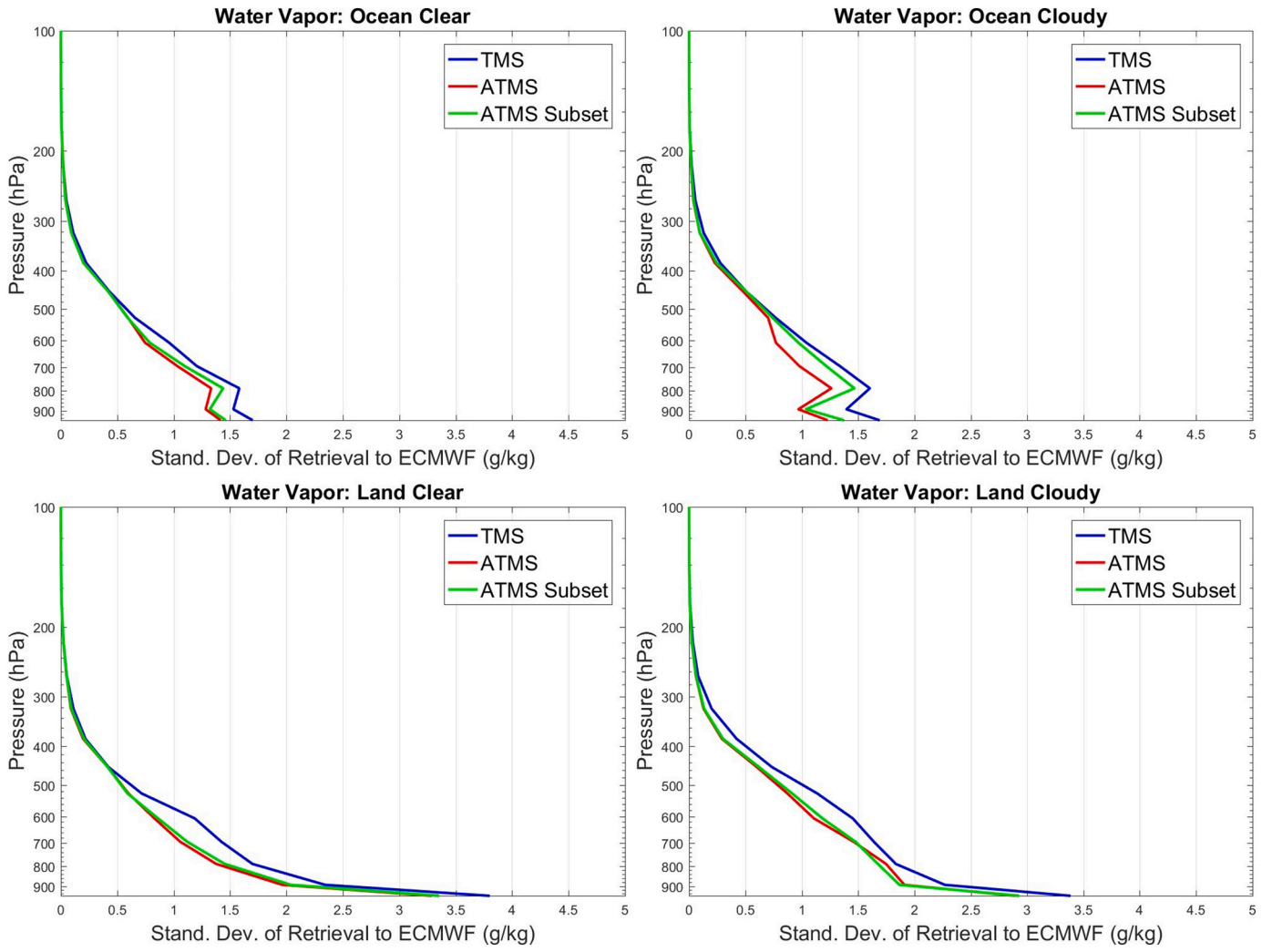

Fig. 9. Water vapor standard deviation of TROPICS, ATMS and ATMS subset referenced to ECMWF under four conditions.

and EUMETSAT. MiRS is in near real-time operation at NOAA/STAR (www.star.nesdis.noaa.gov/mirs). Its applications include monitoring Earth environment, generating the blended total precipitable water and working as one source of temperature information for the Hurricane Intensity and Structure Algorithm at the Cooperative Institute for Research in the Atmosphere (CIRA). We have extended MiRS to add TROPICS into the current microwave sensor family. We have evaluated the humidity and temperature sounding performance which is a core of the mission. We seek to investigate how a CubeSat mission like TROPICS compares against conventional large satellites and whether these new frequencies can provide sounding information comparable to the traditional channels. This is the first study of its kind to examine the humidity and temperature sounding of a CubeSat with F-band and G-band channels. The remainder of the paper proceeds as follows: Section 2 outlines methodology and data including MiRS structure and retrieval scheme. Section 3 presents retrieval results and discussions, where moisture and temperature are examined including the total column water vapor, profiles, and seasonal dependence. We also compare and validate TROPICS Pathfinder retrievals with operational analyses and the Advanced Technology Microwave Sounder (ATMS) on board NOAA-20 (N20). Summary remarks and outlook are presented in the last section.

2. Methods

2.1. Data

TROPICS Pathfinder data has global coverage since it is in a sun-synchronous orbit (approximately 530-km altitude) with a local time of 2 am/pm at ascending and descending nodes, respectively. The early-phase data from August to November 2021 have been released by the TROPICS team and distributed through the NASA Earth Science Data Systems. The data is the provisional Level-1B (L1B) radiance data, which will be further validated and improved. Details about the data structure and L1B calibration can be found in the TROPICS Algorithm Theoretical Basis Document (Leslie and DiLiberto, 2021). The Space Science and Engineering Center (SSEC) at the University of Wisconsin also maintains the TROPICS data at its Data Processing Center, where level-1 radiance and level-2 science products are being processed. TROPICS Pathfinder is the first built unit and uses significantly reworked and even over-tested hardware, and the following CubeSats are expected to have improved performance.

TROPICS TMS has 12 channels at W/F/G bands, including a 92 GHz channel, seven channels near 118 GHz, and four channels near 183 GHz. Fig. 1 shows the weighting functions of these channels derived from a typical tropical profile (Han, 2006). Compared to conventional microwave sounders such as ATMS and AMSU, TROPICS has fewer channels with sparser vertical profiling, which seems to pose a challenge for

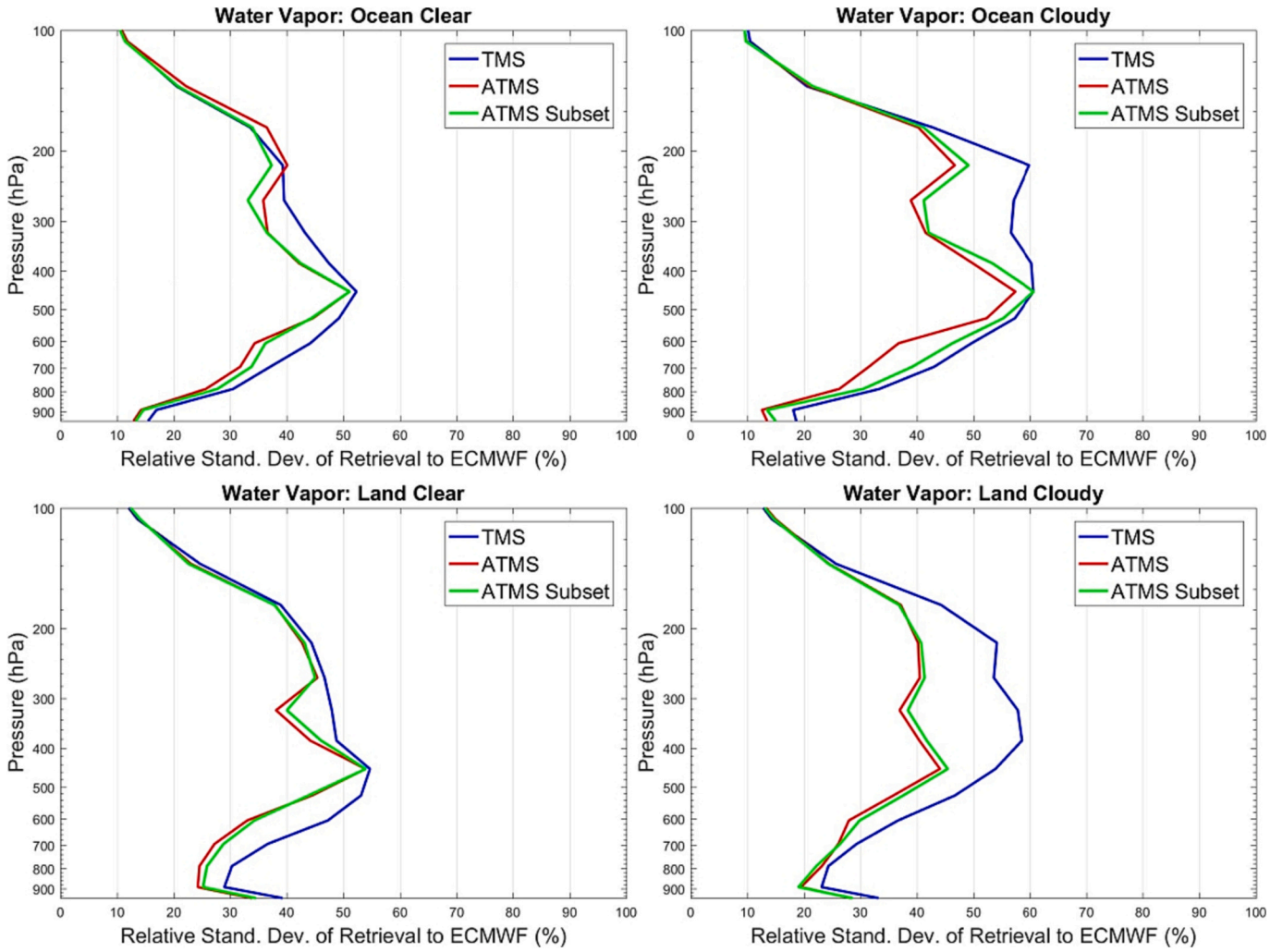

Fig. 10. Water vapor relative standard deviation of TROPICS, ATMS and ATMS subset referenced to ECMWF under four conditions.

retrieval.

Table 1 lists the channel and sensor specification (Blackwell et al., 2018). Also shown are the matchup ATMS channels with similar weighting functions. In spite of a cross-scanning instrument, TROPICS has purely H-pol from channels 1–8 and purely V-pol for channels 9–12, even at off-nadir angles, which is different from conventional cross-track sounders that have a mixed quasi V&H polarization (QV or QH). This is because TROPICS scans by spinning the whole receiver instead of rotating a reflector. The field of view (FOV) size at F-band of TROPICS is smaller (∼24 km) than the counterpart of conventional V-band channels (∼32 km) such as that of ATMS. The measured in-orbit Noise Equivalent Delta Temperature (NEDT) from the four months average is presented in Table 1. The actual NEDT is comparable to the specification. We note that TROPICS F-band NEDT is around 0.6 K, which is higher than ATMS V-band in-orbit NEDT (Kim et al., 2022).

For comparison, NOAA-20 ATMS data are also used. ATMS is a broadband microwave sounder with 22 channels spanning K/Ka/V/W/G bands (Kim et al., 2022). It is currently onboard the Suomi NPP, NOAA-20 & 21 satellites and will also fly on future Joint Polar Satellite System (JPSS) 3–4 satellites. The local equator crossing time of NOAA-20 is 1:30 pm/am for ascending/descending, respectively. The comparison with ATMS can give a sense of TROPICS performance relative to the more traditional sounder systems. Such a comparison can help clarify the relative benefits of a low cost CubeSat mission with the understanding that TROPICS has different and considerably fewer channels and is an Earth Venture mission designed to explore new technologies, but not to replace existing large satellites presently operating. Table 1 shows the matchup channels with similar weighting functions between ATMS and TROPICS. Fig. 2 illustrates the weighting functions of matchup channels under a typical tropical profile. The differences arise from frequencies, polarization, and double (ATMS) and single (TMS) sidebands. Apart from using all ATMS channels, we will also evaluate TROPICS retrievals with a subset of 12 ATMS channels as in the matchup, which permits a more direct comparison of the information content available in the V-band and F-band spectral regions. We detail the experiment setup in the next section.

Other ancillary data include the European Centre for Medium-Range Weather Forecasts (ECMWF) analysis data. The data has a horizontal resolution of 0.25 degrees with 91 vertical layers at the model levels. The analysis is primarily used to evaluate retrievals. It is also used to simulate the top-of-atmosphere brightness temperature (TB) and generate the observation-background (O-B) bias, which is used as the bias correction to reconcile observation and simulation differences. The surface type data for differentiating snow and ice are from the Interactive Multisensor Snow and Ice Mapping System (IMS) developed at the National Snow & Ice Data Center (Helfrich et al., 2007). IMS data help constrain MiRS retrievals with definitive surface types. It is noted that IMS data are only for the Northern Hemisphere. Sea ice in the Southern Ocean, for instance, is unavailable in IMS data.

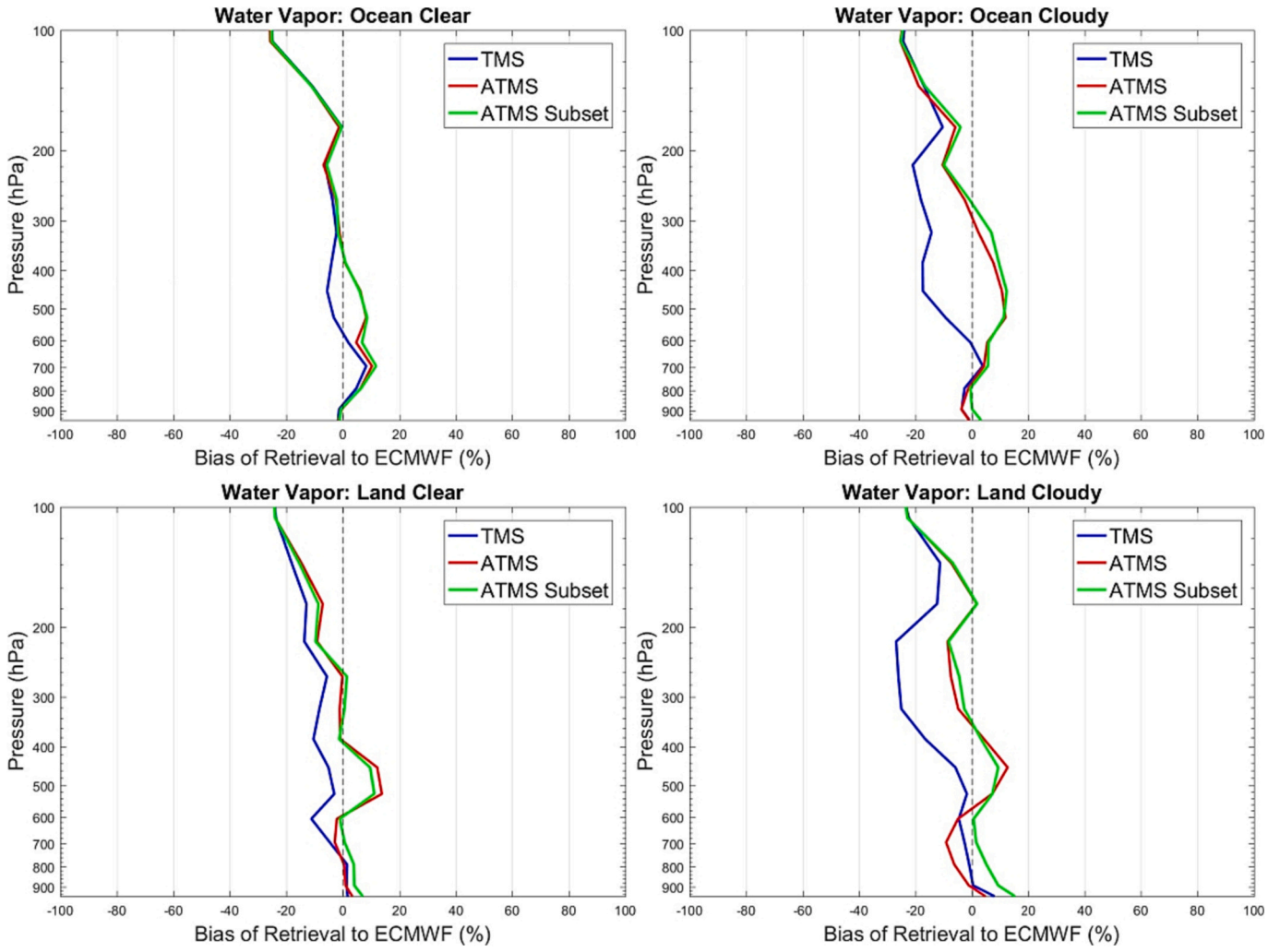

Fig. 11. Water vapor bias of TROPICS, ATMS and ATMS subset referenced to ECMWF under four conditions.

2.2. MiRS configuration

MiRS is the retrieval system supporting a variety of microwave sounders as well as several imagers at NOAA (Boukabara et al., 2011). It has been running operationally and producing retrieval products since 2007. The core of MiRS is based on a 1DVAR retrieval algorithm, solving for a number of atmospheric and surface variables. The cost function to minimize is

$$\mathbf{J}(\mathbf{X}) = \frac{1}{2}(\mathbf{X}-\mathbf{X_0})^T B^{-1}(\mathbf{X}-\mathbf{X_0}) + \frac{1}{2}(\mathbf{Y^m}-\mathbf{Y}(\mathbf{X}))^T E^{-1}(\mathbf{Y^m}-\mathbf{Y}(\mathbf{X})) \quad (1)$$

where $\mathbf{X}$ is the state vector to solve, $\mathbf{X_0}$ is the prior background state from the climatological mean, $\mathbf{Y^m}$ is measured radiance, and $\mathbf{Y}$ is the simulated radiance. $\mathbf{B}$ is the covariance matrix for weighing the state vector, and $\mathbf{E}$ is the covariance matrix representing the measurement noise and modeling error. The minimization of the cost function is iteratively implemented utilizing the derived Jacobian matrix until convergence, which is when the difference between measured and simulated radiances, also known as chi-square, agrees to within a threshold (Boukabara et al., 2011). MiRS uses the Community Radiative Transfer Model (CRTM) as the forward operator, with the Jacobian matrix computed from the tangent linear and adjoint approach (Han, 2006). The first guess in MiRS is from climatological means that are fixed but spatially dependent, with a 5 × 5 degree horizontal resolution and 100 vertical layers. We do not use time-varying analysis data such as ERA5 that coincides with TROPICS observations in time and space as the first guess.

Regarding the ill-conditioned inversion with more unknowns than measured channels, the empirical orthogonal function (EOF) is computed for the background covariance matrix inversion. The eigenvector matrix is truncated to keep the most informative eigenvalue and eigenvectors (for example, the first eight components for temperature and the first four for moisture), and inversion is done in the reduced EOF space. At each iteration, the EOFs computation is implemented back and forth between the geophysical space and the reduced space.

Upon the completion of the 1DVAR retrieval, vertical integration and post-processing are implemented to derive more parameters utilizing retrieved variables. For example, columnar parameters such as the total precipitable water (TPW), ice water path (IWP), graupel water path (GWP), rain water path (RWP), and cloud liquid water (CLW) are computed by vertically integrating relevant retrieved profile variables. There are 100 vertical pressure layers from the ground to 0.01 hPa. Surface rain rate is derived as an empirical function of CLW, RWP and GWP (Liu et al., 2020; Lee et al., 2022). Emissivities post-processing is taken to derive surface products such as snow water equivalent (SWE) and sea ice concentration (SIC). The final MiRS products contain over a dozen of atmospheric and surface parameters. Here we focus on atmospheric humidity and temperature retrievals, since they are of primary importance for microwave sounders and are tied to the core of the TROPICS mission. Precipitation is also a focus of the mission, and we plan to conduct a comprehensive validation of MiRS retrieved precipitation against gauges and other satellite radiometers in a separate study. Kidd et al. (2022) studied TROPICS rainfall with a precipitation retrieval

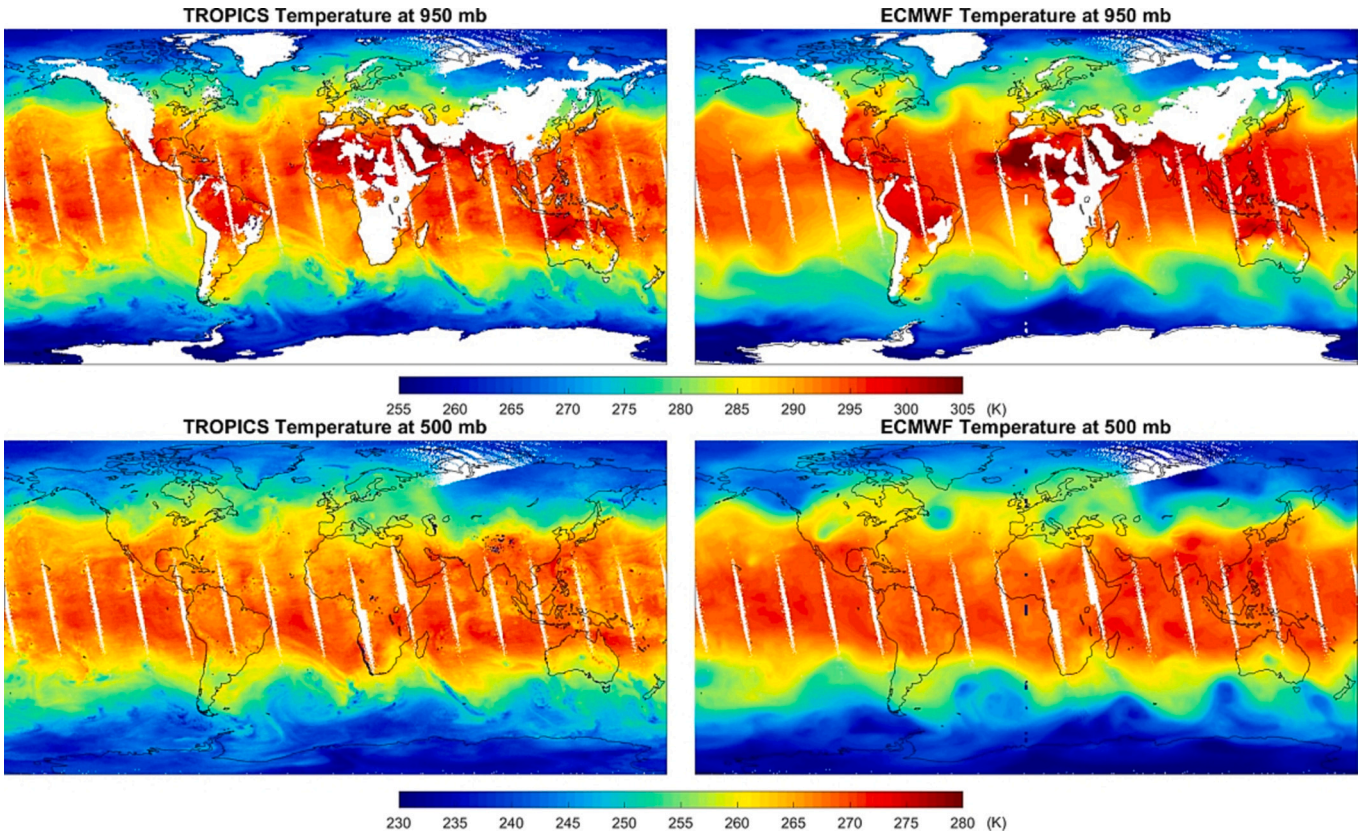

Fig. 12. Retrieved TROPICS temperature at 950 and 500 hPa (left) compared with the ECMWF analysis (right) on 10 October 2021.

algorithm and concluded "In terms of monthly precipitation estimates, the (TROPICS Pathfinder) results fall within the mission specifications and are similar in performance to retrievals from other sounding instruments.".

We have extended MiRS and added TROPICS into the current sensor family. Comprehensive efforts are spent on ingesting the raw TROPICS data, computing static and semi-static parameters such as the surface emissivity covariance matrix, applying bias correction, expanding scripts and validating results. The extension has been successfully tested and verified. For instance, the convergence rate is over 95% with the chi-square generally below one, which is comparable to other sensors such as ATMS (Boukabara et al., 2013). We picked four days, 14 August, 18 September, 11 October, and 9 November 2021, to get the global mean scan-dependent bias correction for each channel, derived from observation minus simulation, which is then applied to every pixel of observations, reconciling observation and RTM modeling. This is a common practice to derive the average bias correction, keeping most of the data independent from deriving the bias correction. The picked dates are relatively random. We tried to use the same date interval, provided they do not have many data gaps due to maneuvers or other in-orbit tests. Data from the other days are used for independent verification. The entire early-phase data have been retrieved and analyzed.

We have compared TROPICS with N20 ATMS. Two experiments of ATMS are conducted: one with all the 22 channels of ATMS, and the other uses a subset of 12 channels that have similar weighting functions of TROPICS, as shown in Table 1 and Fig. 2. This second experiment reduces the sensor difference and provides insights into comparing F-band and V-channels. We also looked at other sensors such as Suomi NPP ATMS and MetOp B&C AMSU-A & MHS, which exhibit similar performance as N20 ATMS and thus are not presented here.

3. Results and discussion

3.1. TROPICS channel sensitivity

One appealing innovation of TROPICS is the use of new frequencies at F-band and 205 GHz, which are distinct from the V-band and upper-bound 190 GHz at G-band of conventional microwave sounders. Fig. 3 shows a snapshot of the super Typhoon Mindulle captured by TROPICS. The highlight is the large brightness temperature (TB) dynamic range of 155 degrees at 205 GHz, ranging from 133 to 288 K. In comparison, the 190 GHz channel has a dynamic range of 129 K from 148 to 277 K. The FOV size of 205 GHz is 15.2 km, which is smaller but comparable to 190 GHz (16.9 km). The 205-GHz perceives finer structures of the typhoon: the Mindulle eye and the scattered rainbands are clearly resolved.

We look into the brightness temperature sensitivity as a function of MiRS retrieved parameters. The coincident channels of NOAA-20 ATMS, with similar weighting functions shown in Fig. 2, are compared against TROPICS. Retrieval results of NOAA-20 and TROPICS data on the same day are compared with over two million samples. We classify the data into subsets over the ocean and land. Since IMS surface type classification is unavailable for the Southern Hemisphere and snow and sea ice are relatively inaccurate, we analyze data with a latitude range from −50 to 50 degrees.

Fig. 4 illustrates the TB against the retrieved rain rate. The highlight is that TROPICS F-band and 205 GHz exhibit pronounced sensitivity to rain rate: TB decreases as rain rate rises up. The counterpart frequency of ATMS V-band is relatively flat and less sensitive to rain. For instance, TROPICS channel 3 of 115 GHz and ATMS channel 4 of 52.8 GHz have a close TB of ~256 K over the ocean when the rain rate is very low at 1 mm/h. As the rain rate rises up to 14 mm/h, TROPICS TB decreases by 50 K, but ATMS TB is almost the same with less than 5 K variation. F-band is overall much more sensitive to rain. TROPICS 190 and 205 GHz have a TB drop of 60 and 80 K, respectively. ATMS 165 GHz is 10–20 K

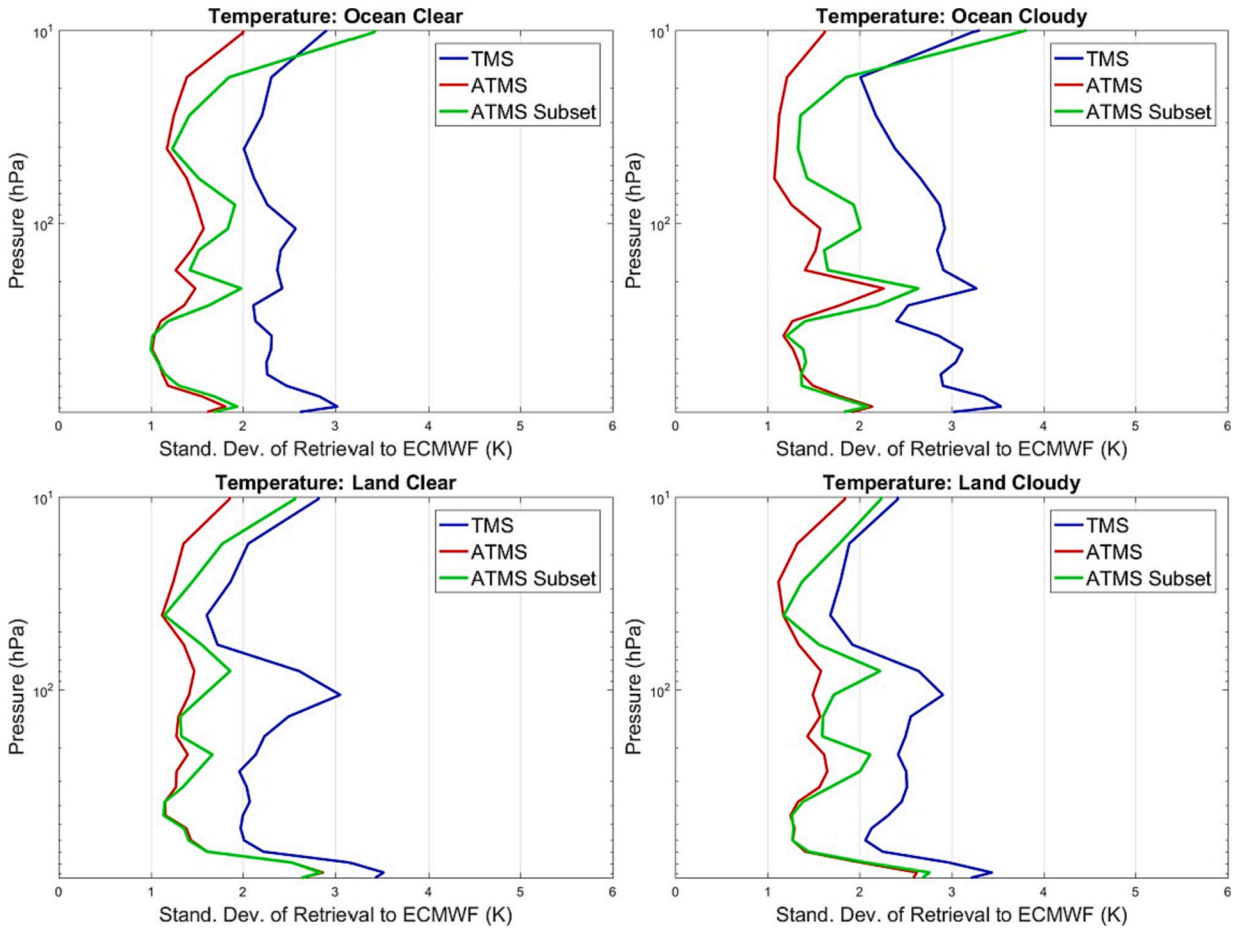

Fig. 13. Temperature standard deviation of TROPICS, ATMS and ATMS subset referenced to ECMWF under four conditions.

warmer than TROPICS 205 GHz. The 205 GHz shows more scattering to rain rate. This is consistent with the typhoon Mindulle case, where the TB range difference between 190 and 205 GHz is 26 K (Fig. 2).

The TB sensitivity to the total precipitable water (TPW) is shown in Fig. 5. TPW is the integration of columnar water vapor in the atmosphere. It is a critical variable for representing Earth water vapor and estimating the greenhouse effect, and therefore routinely produced from many satellites (Grody et al., 2001; Lee et al., 2022). The relationship between TB and TPW is more complex as it is coupled with surface emission, water vapor absorption/emission, and hydrometeor scattering. At W-band of around 90 GHz, TROPICS and ATMS exhibit similar sensitivity, with a remarkable TB increase along TPW over the ocean but relatively flat over land. This is due to the much colder oceanic emission than land, with a ~60 K difference in surface emission. Over the ocean, water vapor appears warmer and more TPW tends to increase the TB.

At the TROPICS F-band of channels 2–6, TB also increases with TPW over the ocean. The weighting functions of these channels peak in the troposphere, and more warm moisture tends to increase the TB. The over-land TB has less increase due to warm land emissions. On the other hand, TB decreases with TPW for channels 7–8 at F-band. The weighting functions of the two channels are very high, reaching or exceeding the tropopause. The atmosphere becomes more opaque at the two channels, which are less sensitive lower troposphere emissions. Rather, larger TPW corresponds to regions with denser atmospheres, where the two channels see more upper and colder troposphere emissions.

At F-band, TROPICS shows different sensitivity to TPW against corresponding ATMS channels. One reason is that F-band and V-band frequencies are quite different with different weighting functions. For G-band, TROPICS and ATMS are similar due to closer frequencies. The 205 GHz exhibits a noticeable difference compared with 165 GHz. When TPW gets larger, TROPICS TMS TB is mostly lower than ATMS since hydrometeors like clouds give rise to absorption and scattering.

The TB sensitivity shows pronounced contrast between TROPICS and ATMS, particularly regarding F-band and 205 GHz. Some of the difference has been investigated in previous studies, primarily by theoretical simulation (Bauer et al., 2005; Mahfouf et al., 2015). The only observation-based is through the MWHS-2 on board the large satellite FY-3C&D&E (Lawrence et al., 2018; Mao et al., 2022). The distinct sensitivity of TROPICS can pose challenges for profile retrieval, but more interestingly, it also means new information content at these channels. We will show the retrieval results in the following sections.

3.2. *Water vapor sounding*

The water vapor sounding results are presented in this section. Fig. 6 shows a one-day (10 October 2021) comparison of MiRS-produced TROPICS TPW against that of ECMWF analysis. The retrieval well captures TPW features as verified by the collocated ECMWF TPW. Highest TPW is found in the Intertropical Convergence Zone (ITCZ) and the South Pacific convergence zone (SPCZ). Atmospheric rivers in mid-latitude regions of the Atlantic and Pacific oceans can be seen. Over land, low TPW is perceived over the Tibetan Plateau, Andes, and Rocky mountains. Very low TPW in Greenland and Antarctica is obvious. Overall, the retrieved TPW is successful over different surface types.

A quantitative statistical validation is shown in Fig. 7. TROPICS TPW is compared with ECMWF under clear and cloudy conditions. The cloudy condition is defined by the retrieved cloud liquid water (CLW) larger than 0.05 mm. The correlation coefficient is very high of 0.967 and 0.958 under clear and cloudy conditions, respectively. TROPICS TPW is slightly larger than ECMWF with a bias of 0.82 and 1.40, while the

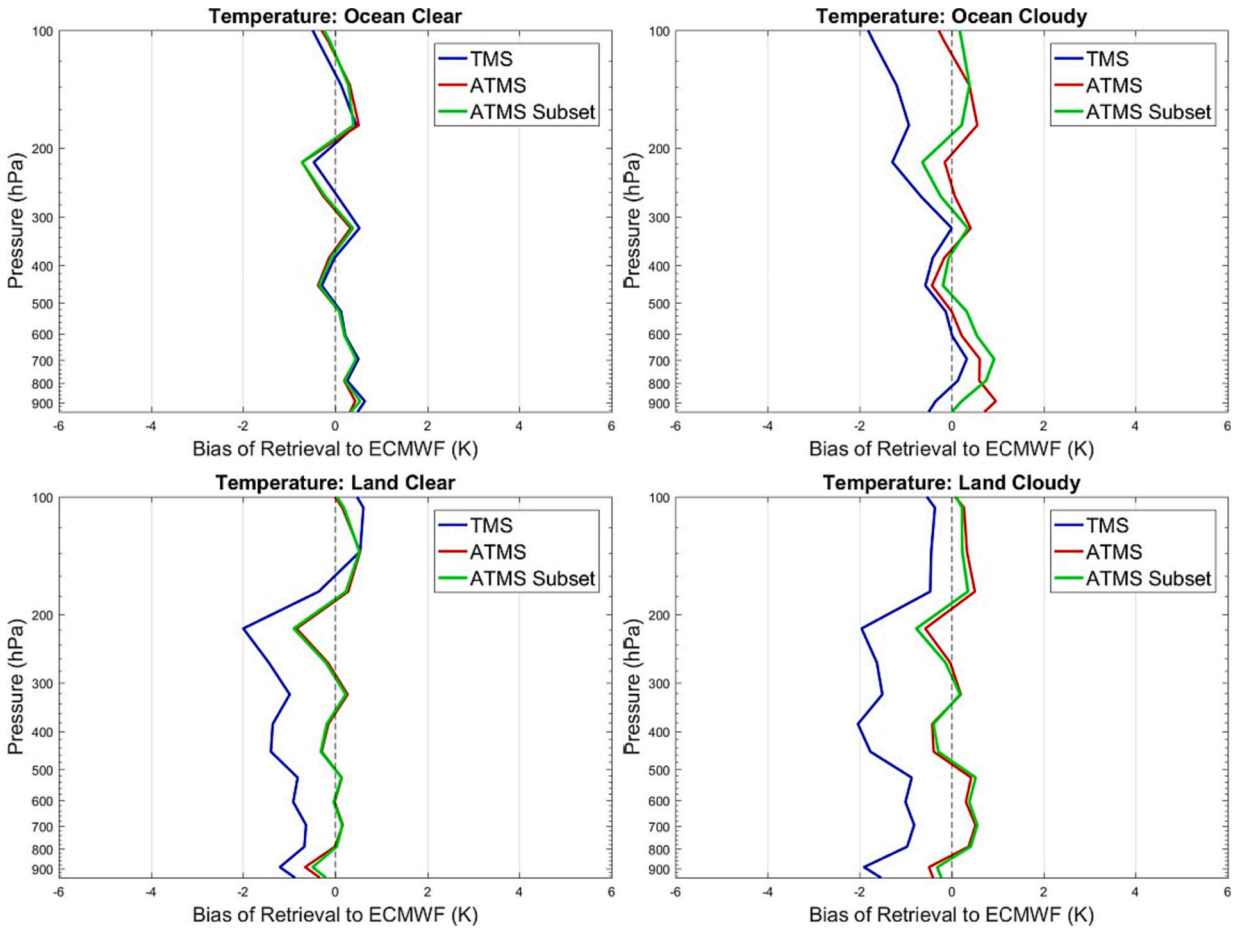

Fig. 14. Temperature bias of TROPICS, ATMS and ATMS subset referenced to ECMWF under four conditions.

standard deviation is 4.14 and 4.37, respectively. There is a slight degradation of retrieval when it is cloudy, which is similar to other microwave sounders (Boukabara et al., 2011).

Table 2 shows the TPW statistics, and the results from two additional experiments of ATMS and ATMS subset are also presented for comparison. The sample numbers under clear and cloudy conditions are close, indicating similar retrieval performance on discriminating clouds. The correlation coefficients are over 0.95 for all experiments. There is a slight degradation under cloudy conditions compared to clear conditions. Using all ATMS channels outperforms subsetting ATMS channels, which is not unexpected and highlights the advantage of using more channels to improve retrievals. The performance of the ATMS subset, which matches up with TROPICS TMS channels, is still slightly better than TMS, as shown in terms of correlation and standard deviation. We will discuss this after presenting the other results.

Examples of water vapor at specific pressure levels are illustrated in Fig. 8. The water vapor spatial distributions at the 950 and 500 hPa are shown between TROPICS and ECMWF. At 950 hPa, there are no data in mountain areas due to their high elevation of low pressure. The spatial patterns of water vapor are consistent between TROPICS and ECMWF. As the pressure decreases, water vapor amount is reduced.

Figs. 9 and 10 show the comparison of water vapor vertical profiles to ECMWF in terms of absolute and relative standard deviation, respectively. The absolute standard deviation, i.e. standard deviation, is the standard deviation of the retrieved parameter minus that of ECMWF. The relative standard deviation is in the unit of percentage, which is the absolute standard deviation divided by the average ECMWF parameter at each pressure level. Since water vapor exponentially decreases along the altitude, the relative standard deviation with the percentage profile complements the standard deviation. The results are classified into four scenarios of ocean clear, ocean cloudy, land clear, and land cloudy conditions for three experiments of TMS, ATMS, and ATMS subset. Regarding standard deviation, the retrieval shows near-surface (>800 hPa) degradation over land compared to over the ocean. This is not a surprise since land emission is more complex. Oceanic retrievals are similar under clear and cloudy conditions, which is in contrast with land which is more degraded in cloudy conditions except near the surface. TROPICS TMS is degraded compared to ATMS and ATMS subset, with an overall standard deviation of 0.93, 0.76, and 0.80 g/kg from surface to 100 hPa for the three experiments, respectively. ATMS subset is degraded compared to ATMS, as expected.

While the standard deviation of water vapor decreases along altitude, the relative standard deviation shows a larger percentage deviation in the middle troposphere from 700 to 200 hPa, which can be as high as 50% and exceeds that on the surface. Overall, the retrieval performance ranks from high to low in the order of ATMS, ATMS subset, and TMS. Under cloudy land conditions, TMS shows a large relative standard deviation as high as 58%. Under the other three scenarios, TMS is closer to ATMS and ATMS subset. The retrieval performance is related to surface type and cloud. For example, the land-cloudy scenario exhibits degraded performance near the surface but an improvement from 700 to 200 hPa, compared to the ocean-cloudy condition. The reason for this can be multifold. When cloudy, the land surface emission weighs less, i.e., the weighting function lifts up, facilitating retrievals in the atmosphere. Regarding ATMS and TMS differences, the F-band is of higher frequency and is affected more by hydrometers than V-band. Such sensitivity can affect temperature retrieval: since moisture and temperature are coupled a better representation of temperature improves moisture retrieval. We will present temperature results including vertical profiles in Section 3.3.

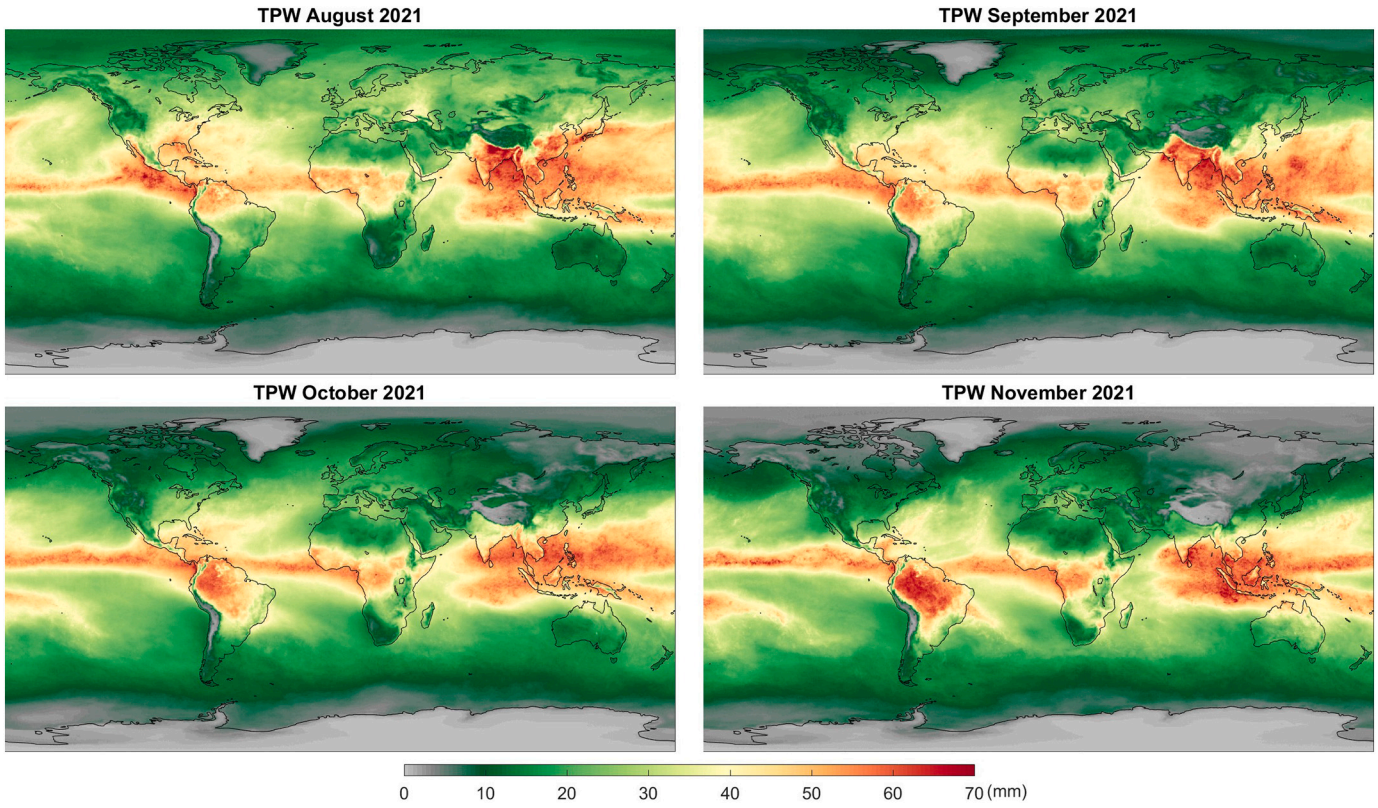

Fig. 15. Monthly TROPICS TPW. The spatial distribution and seasonality are well captured.

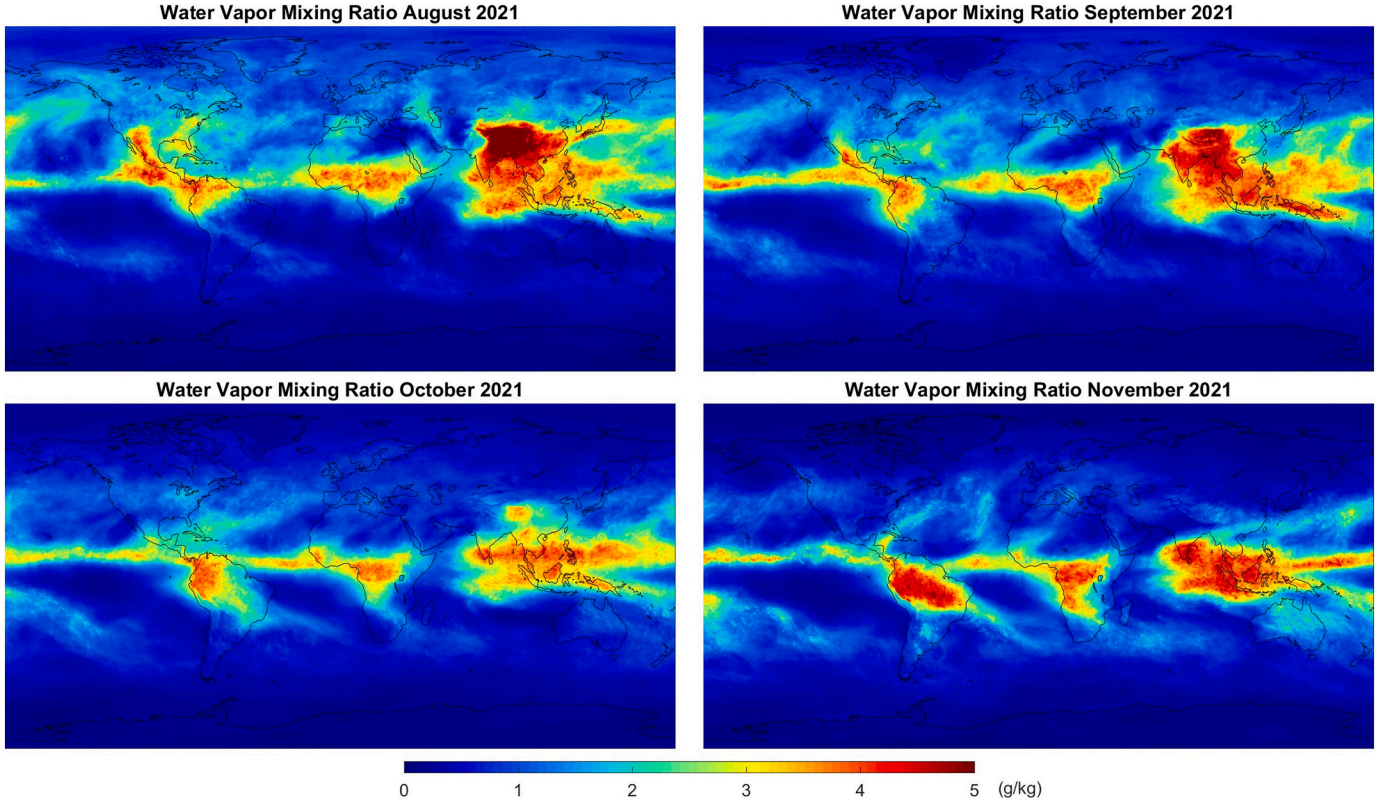

Fig. 16. Monthly TROPICS water vapor mixing ratio at 500 hPa.

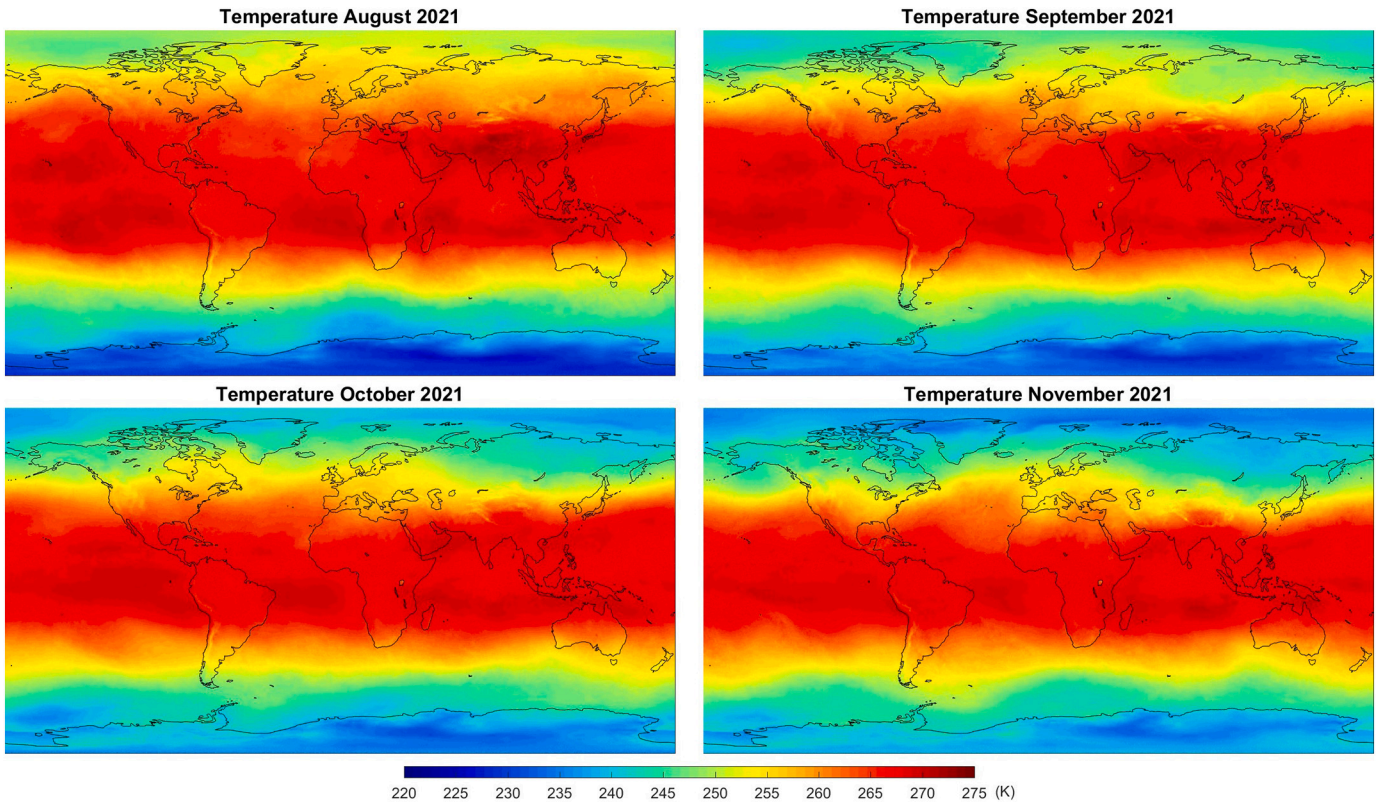

Fig. 17. Monthly TROPICS temperature at 500 hPa.

Fig. 11 presents the mean bias of water vapor compared to ECMWF. Compared to standard deviation, the mean bias is a secondary but also a basic metric for evaluating retrieval quality. Overall, the characterization of bias under the four scenarios is similar to standard deviation. We note that the bias leans to be more negative in cloudy conditions for TROPICS, which again implies the impact of cloud on retrieval.

3.3. Temperature sounding

Fig. 12 shows an example of atmospheric temperature sounding. The temperature spatial distribution at 950 and 500 hPa are demonstrated for TROPICS and ECMWF, respectively. The unavailable temperature retrievals in places such as the Tibetan Plateau at 950 hPa are due to the elevation since the surface pressure in regions such as mountains is less than 950 hPa. The near-surface temperature is well retrieved compared to ECMWF. High air temperature is seen in the Sahara desert, Amazon rainforest, and northern Australia. Over the ocean, the temperature decrease from tropics to poles is also well reproduced.

The temperature profiles against ECMWF are illustrated in Figs. 12 (standard deviation) and 13 (bias). Overall, the standard deviation of temperature is like water vapor, with ATMS the smallest, followed by ATMS subset and then TMS. Also, retrieval is dependent on surface type and clouds. The near-surface performance is degraded over land than over the ocean, while the degradation in the upper atmosphere is not significant. Clouds also degrade retrieval. TROPICS TMS has a mean average standard deviation of 2.36, 2.83, 2.37, and 2.45 K from surface to 10 hPa under ocean-clear, ocean-cloudy, land-clear, and land-cloudy conditions, respectively. By contrast, ATMS is 1.35, 1.49, 1.69, and 1.68 K, while ATMS subset is 1.46, 1.73, 1.72, and 1.82 K, under the four scenarios, respectively. In Fig. 14, we see TMS bias is similar to ATMS and ATMS subset under ocean-clear conditions but gets more negatively biased with clouds or over land. This seems to be coupled with water vapor, where negative bias is also found over land. Temperature and moisture are simultaneously retrieved in the 1DVar retrieval, and a degraded temperature affects moisture retrieval. In the meantime, there could be room for improving F-band retrieval by mitigating the bias and optimizing the retrieval algorithm.

3.4. Monthly TPW, water vapor and temperature

The monthly TROPICS TPW is shown in Fig. 15. Although not shown here, the TROPICS TPW agrees very well compared with ECMWF, with daily correlation coefficients generally over 0.94. The spatial distribution of TPW features a clear equator-to-pole gradient with high amounts in tropical regions. Over the ocean, high TPW is noted in persistent convective and cloudy areas such as the tropical west Pacific Ocean and east Indian Ocean. The ITCZ and SPCZ are noticeable with high TPW. Over land regions such as Amazon, Congo basin and Indonesian Maritime Continent, TPW is also abundant due to coupling convergence and continental meteorological factors. The surface elevation affects TPW, showing lower TPW associated with higher elevation. Persistent low TPW can be found in the Himalayas, Andes, Rocky Mountains, and East Africa.

The seasonal variability of TPW is remarkable from August to November. In the Northern Hemisphere, the transition of TPW from high to low amounts is obvious. Particularly, areas of North Asia, Canada and the Tibetan Plateau quickly dry up. In the Southern Hemisphere, high TPW quickly builds up over the Amazon basin, South Africa, etc. The ITCZ movement toward the south is also pronounced. Overall, the TPW shifts toward the south in southern summer.

The monthly mean water vapor mixing ratio and temperature at 500 hPa are illustrated in Figs. 16 and 17. While water vapor at 500 hPa has similarity to TPW, with gradients from the equator to poles, there is a striking difference in regions such as the Himalayas. In August and September, the water vapor values are very high in the Himalayas, which is different from the low TPW there. This is mainly due to the surface elevation, which lifts air and moisture. Although the columnar TPW is low in these regions, the moisture is increased at 500 hPa. In

southern summer, Amazon, Congo The temperature distribution at 500 hPa also transitions from high to low values with an equator-to-pole gradient. In contrast to the near-surface temperature correlated with surface types and elevation, 500 hPa temperature is more uniformly distributed over the ocean and land, as it is of the higher altitude in the middle troposphere. But regions such as the Himalayas still stand out from the temperature anomaly due to the impact of very high elevation.

4. Concluding remarks

Atmospheric humidity and temperature sounding from TROPICS Pathfinder have been investigated through the MiRS retrieval system. TROPICS is a novel mission and the first CubeSat with channels at F-band and 205 GHz, offering a new perspective for moisture and temperature sounding. We have examined TROPICS early-phase data from its Pathfinder and performed retrieval with MiRS, a physically-based inversion algorithm. We have extended MiRS to add TROPICS processing capability, and the retrieval is successful and verified. Comparison and validation against analyses and NOAA-20 ATMS were conducted, including an ATMS subsetting experiment with retrieval implemented with a subset of matchup channels.

The quality of TROPICS moisture and temperature retrievals is encouraging. TROPICS captures well the dynamics, spatial distribution, and seasonal variability of moisture and temperature. The retrieved TPW compared with ECMWF has a correlation coefficient of 0.955, 0.985, and 0.977 for TROPICS TMS, ATMS, and ATMS subset, respectively. For the water vapor profile, the standard deviation of retrieval to ECMWF is 0.93, 0.76, and 0.80 g/kg for TROPICS TMS, ATMS, and ATMS subset, respectively. Regarding temperature, the standard deviation is 2.5, 1.5, and 1.6 K for the three experiments, respectively. Clouds and land degrade retrievals compared to the ocean and clear conditions. V-band appears to be less affected by hydrometeors, resulting in better temperature retrieval and moisture, as the two parameters are coupled. The lower noise of ATMS also favors better retrievals.

The new F-band and 205 GHz of TROPICS appear to bring in new information content for atmospheric sounding. The retrieval results reveal distinct TB sensitivity to water vapor and hydrometeors between TROPICS and ATMS. Specifically, the F-band exhibits remarkable sensitivity to rain rate compared to V-band, where the TB can drop dramatically as much as 50 K with the rain rate increase, contrasting to less than 5 K variation at the counterpart channel at V-band. That is, the sensitivity is 20 times higher at specific channels, suggesting that temperature sounding may be impacted by the presence of precipitation. The 205 GHz channel measurements exhibit over 20 K greater dynamic range than 190 GHz channel measurements, and are colder than ATMS measurements at 165 GHz in the presence of hydrometeors; finer features of the hurricane eye and rainbands are also better resolved. The TB sensitivity to TPW at F-band and 205 GHz is also different from V-band and 165/190 GHz. The results highlight that F-band and 205 GHz have potential new information content, which can be useful for studying cloud ice, snow, and arctic weather.

As the TROPIC Pathfinder continues collecting data and follow-on CubeSats are on the way toward a more complete constellation, we look forward to further exploring TROPICS potential. The extension of MIRS allows for analyzing extensive data in an automated way. MiRS is able to retrieve more geophysical variables such as hydrometeors, surface parameters, and rainfall in addition to moisture and temperature. Future investigation will include more extensive retrievals, comparisons, and potential insights. With more TROPICS CubeSats in orbit, the diurnal variations and even finer weather dynamics can be examined.

CRediT authorship contribution statement

John Xun Yang: Conceptualization, Software, Visualization, Formal analysis, Writing - review & editing. **Yong-Keun Lee:** Conceptualization, Software, Formal analysis, Writing - review & editing. **Christopher Grassotti:** Conceptualization, Formal analysis, Writing - review & editing. **Kevin Garrett:** Formal analysis, Writing - review & editing. **Quanhua Liu:** Conceptualization, Formal analysis, Writing - review & editing. **William Blackwell:** Conceptualization, Formal analysis, Writing - review & editing. **R. Vincent Leslie:** Formal analysis, Writing - review & editing. **Tom Greenwald:** Formal analysis, Writing - review & editing. **Ralf Bennartz:** Formal analysis, Writing - review & editing. **Scott Braun:** Formal analysis, Writing - review & editing.

Declaration of Competing Interest

The authors declare that they have no known competing financial interests or personal relationships that could have appeared to influence the work reported in this paper.

Data availability

Data will be made available on request.

Acknowledgment

The manuscript contents are solely the opinions of the authors and do not constitute a statement of policy, decision, or position on behalf of NOAA or the U.S. government. This work is supported by National Oceanic and Atmospheric Administration (NOAA) under grant NA19NES4320002 to the Cooperative Institute for Satellite and Earth system Studies (CISESS) at the University of Maryland/Earth System Science Interdisciplinary Center (ESSIC).

References

Bauer, P., Moreau, E., Di Michele, S., 2005. Hydrometeor retrieval accuracy using microwave window and sounding channel observations. J. Appl. Meteorol. 44, 1016–1032.

Blackwell, W.J., 2015. The micromas and mirata cubesat atmospheric profiling missions. In: 2015 IEEE MTT-S International Microwave Symposium. IEEE, pp. 1–3.

Blackwell, W.J., Braun, S., Bennartz, R., Velden, C., DeMaria, M., Atlas, R., Dunion, J., Marks, F., Rogers, R., Annane, B., et al., 2018. An overview of the tropics nasa earth venture mission. Q. J. R. Meteorol. Soc. 144, 16–26.

Boukabara, S.A., Garrett, K., Chen, W., Iturbide-Sanchez, F., Grassotti, C., Kongoli, C., Chen, R., Liu, Q., Yan, B., Weng, F., et al., 2011. Mirs: An all-weather 1dvar satellite data assimilation and retrieval system. IEEE Trans. Geosci. Remote Sens. 49, 3249–3272.

Boukabara, S.A., Garrett, K., Grassotti, C., Iturbide-Sanchez, F., Chen, W., Jiang, Z., Clough, S., Zhan, X., Liang, P., Liu, Q., et al., 2013. A physical approach for a simultaneous retrieval of sounding, surface, hydrometeor, and cryospheric parameters from snpp/atms. J. Geophys. Res.: Atmos. 118, 12–600.

Camps, A., Golkar, A., Gutierrez, A., De Azua, J.R., Munoz-Martin, J.F., Fernandez, L., Diez, C., Aguilella, A., Briatore, S., Akhtyamov, R., et al., 2018. Fsscat, the 2017 copernicus masters' "esa sentinel small satellite challenge" winner: A federated polar and soil moisture tandem mission based on 6u cubesats. In: IGARSS 2018–2018 IEEE International Geoscience and Remote Sensing Symposium. IEEE, pp. 8285–8287.

Crews, A., Blackwell, W.J., Leslie, R.V., Grant, M., Osaretin, I.A., DiLiberto, M., Milstein, A., Leroy, S., Gagnon, A., Cahoy, K., 2020. Initial radiance validation of the microsized microwave atmospheric satellite-2a. IEEE Trans. Geosci. Remote Sens. 59, 2703–2714.

D'Addio, S., Kangas, V., Klein, U., Loiselet, M., Mason, G., 2014. The microwave radiometers on-board metop second generation satellites. In: 2014 IEEE Metrology for Aerospace (MetroAeroSpace). IEEE, pp. 599–604.

Geer, A., Baordo, F., Bormann, N., Chambon, P., English, S., Kazumori, M., Lawrence, H., Lean, P., Lonitz, K., Lupu, C., 2017. The growing impact of satellite observations sensitive to humidity, cloud and precipitation. Q. J. R. Meteorol. Soc. 143, 3189–3206.

Grody, N., Zhao, J., Ferraro, R., Weng, F., Boers, R., 2001. Determination of precipitable water and cloud liquid water over oceans from the noaa 15 advanced microwave sounding unit. J. Geophys. Res.: Atmos. 106, 2943–2953.

Han, Y., 2006. Jcsda community radiative transfer model (crtm): Version 1.

Helfrich, S.R., McNamara, D., Ramsay, B.H., Baldwin, T., Kasheta, T., 2007. Enhancements to, and forthcoming developments in the interactive multisensor snow and ice mapping system (ims). Hydrol. Process.: Int. J. 21, 1576–1586.

Joo, S., Eyre, J., Marriott, R., 2013. The impact of metop and other satellite data within the met office global nwp system using an adjoint-based sensitivity method. Mon. Weather Rev. 141, 3331–3342.

Kan, W., Han, Y., Weng, F., Guan, L., Gu, S., 2020. Multisource assessments of the fengyun-3d microwave humidity sounder (mwhs) on-orbit performance. IEEE Trans. Geosci. Remote Sens. 58, 7258–7268.

Kidd, C., Matsui, T., Blackwell, W., Braun, S., Leslie, R., Griffith, Z., 2022. Precipitation estimation from the nasa tropics mission: Initial retrievals and validation. Remote Sens. 14, 2992.
Kidder, S.Q., Goldberg, M.D., Zehr, R.M., DeMaria, M., Purdom, J.F., Velden, C.S., Grody, N.C., Kusselson, S.J., 2000. Satellite analysis of tropical cyclones using the advanced microwave sounding unit (amsu). Bull. Am. Meteorol. Soc. 81, 1241–1260.
Kim, E., Abraham, S., Amato, J., Blackwell, W.J., Cho, P., Fuentes, J., Hernquist, M., Kam, J., Leslie, R.V., Liu, Q., et al., 2022. An evaluation of noaa-20 atms instrument pre-launch and on-orbit performance characterization. IEEE Trans. Geosci. Remote Sens. 60, 1–13.
Kunkel, K.E., Changnon, S.A., Reinke, B.C., Arritt, R.W., 1996. The July 1995 heat wave in the midwest: A climatic perspective and critical weather factors. Bull. Am. Meteorol. Soc. 77, 1507–1518.
Lagaune, B., Berge, S., Emrich, A., 2021. Arctic weather satellite, a microsatellite constellation for improved weather forecasting in arctic and globally.
Lawrence, H., Bormann, N., Geer, A.J., Lu, Q., English, S.J., 2018. Evaluation and assimilation of the microwave sounder mwhs-2 onboard fy-3c in the ecmwf numerical weather prediction system. IEEE Trans. Geosci. Remote Sens. 56, 3333–3349.
Lee, Y.K., Grassotti, C., Liu, Q., Liu, S.Y., Zhou, Y., 2022. In-depth evaluation of mirs total precipitable water from noaa-20 atms using multiple reference data sets. Earth Space Sci. 9, e2021EA002042.
Leslie, R.V., DiLiberto, M., 2021. Time-resolved observations of precipitation structure and storm intensity with a constellation of smallsats: Level-1 radiance algorithm theoretical basis document.https://ntrs.nasa.gov/citations/20210018919.
Levin, N., Heimowitz, A., 2012. Mapping spatial and temporal patterns of mediterranean wildfires from modis. Remote Sens. Environ. 126, 12–26.
Liu, S., Grassotti, C., Liu, Q., Lee, Y.K., Honeyager, R., Zhou, Y., Fang, M., 2020. The noaa microwave integrated retrieval system (mirs): Validation of precipitation from multiple polar-orbiting satellites. IEEE J. Select. Top. Appl. Earth Obs. Remote Sens. 13, 3019–3031.
Mahfouf, J.F., Birman, C., Aires, F., Prigent, C., Orlandi, E., Milz, M., 2015. Information content on temperature and water vapour from a hyper-spectral microwave sensor. Q. J. R. Meteorol. Soc. 141, 3268–3284.
Mao, J., Qin, Z., Li, J., Han, Y., Huang, J., 2022. Performance evaluation and noise mitigation of the fy-3e microwave humidity sounder. Remote Sens. 14, 4835.
Marinan, A.D., Cahoy, K.L., Bishop, R.L., Lui, S.S., Bardeen, J.R., Mulligan, T., Blackwell, W.J., Leslie, R.V., Osaretin, I.A., Shields, M., 2016. Assessment of radiometer calibration with gps radio occultation for the mirata cubesat mission. IEEE J. Select. Top. Appl. Earth Obs. Remote Sens. 9, 5703–5714.
Padmanabhan, S., Gaier, T.C., Tanner, A.B., Brown, S.T., Lim, B.H., Reising, S.C., Stachnik, R., Bendig, R., Cofield, R., 2020. Tempest-d radiometer: Instrument description and prelaunch calibration. IEEE Trans. Geosci. Remote Sens. 59, 10213–10226.
Saunders, R.W., Hewison, T.J., Stringer, S.J., Atkinson, N.C., 1995. The radiometric characterization of amsu-b. IEEE Trans. Microw. Theory Tech. 43, 760–771.
Yang, J.X., You, Y., Blackwell, W., Liu, Q., Ferraro, R., Draper, D., Atkinson, N., Hewison, T., Misra, S., Peng, J., 2022. An adaptive calibration window for noise reduction of satellite microwave radiometers. IEEE Trans. Geosci. Remote Sens.
Yang, Z., Lu, N., Shi, J., Zhang, P., Dong, C., Yang, J., 2012. Overview of fy-3 payload and ground application system. IEEE Trans. Geosci. Remote Sens. 50, 4846–4853.